Molecular beam epitaxy of InSb on Si substrates using fluoride buffer layers

W. K. Liu,[a] J. Winesett, Weiluan Ma, Xuemei Zhang, and M. B. Santos
Department of Physics and Astronomy and Laboratory for Electronic Properties of Materials, University of Oklahoma, Norman, Oklahoma 73019

X. M. Fang and P. J. McCann
School of Electrical Engineering and Laboratory for Electronic Properties of Materials, University of Oklahoma, Norman, Oklahoma 73019

(Received 4 September 1996; accepted for publication 8 November 1996)

The molecular beam epitaxy of InSb/Si structures was accomplished using group IIa fluoride buffer layers. InSb growth was initiated by opening the In and Sb shutters simultaneously at substrate temperatures between 300 °C and 400 °C, producing In-terminated InSb(111)-A surfaces on CaF_2/Si(111) substrates. Reflection high-energy electron diffraction, electron channeling, and high resolution x-ray diffraction measurements indicated that the InSb layers were of good crystalline quality. Electron mobilities at room temperature were as high as 65 000 cm^2/V s for an 8-μm-thick InSb layer grown on CaF_2/Si(111). On CaF_2/Si(001) substrates, the InSb layers grew in the (111) orientation with two domains 90° apart. These InSb layers and ones grown on BaF_2/CaF_2/Si(111) substrates exhibited inferior electrical and structural properties compared to structures grown on CaF_2/Si(111) substrates. © *1997 American Institute of Physics.* [S0021-8979(97)02904-6]

I. INTRODUCTION

InSb has the smallest band gap, highest intrinsic electron mobility, and lowest electron effective mass of all binary III-V compounds. These characteristics make InSb-based structures candidates for infrared devices, high speed transistors, and magnetic field sensors. Although there is a large lattice mismatch with InSb, Si is still an attractive substrate material because Si integrated circuit technology is very mature and low-cost, rugged, large-area Si wafers are readily available. With advancements in molecular beam epitaxy (MBE) technology, heteroepitaxy has been achieved on Si substrates with a lattice mismatch as large as 20%.[1–12] Monolithic integration of InSb devices on Si substrates would offer advantages in microelectronics and infrared detector array fabrication.

Compared to the growth of GaAs (~4% mismatch) and CdTe (~19% mismatch) on Si, much less has been reported on the heteroepitaxy of InSb on Si.[8–13] The large lattice mismatch (>19%), the different thermal expansion coefficients ($\alpha_{InSb} \approx 2\alpha_{Si}$ @300 K) and antiphase domain (APD) formation (polar on nonpolar growth for (001) and (111) orientations) all present challenges. Some problems have been alleviated using tilted substrates,[9–11] In pre-deposition[8] and the insertion of various buffer layers.[8,10–14] Group IIa fluoride layers have been widely used as buffers for the growth on Si of PbSe[7,15,16] and CdTe,[1–3] whose lattice constant is close to that of InSb. As evident from Fig. 1, the ~19% lattice mismatch between InSb and Si can be reduced through graded layers of CaF_2 and BaF_2.

MBE growth of high quality CaF_2 and BaF_2 films on Si substrates has been demonstrated by several groups.[17] The CaF_2/Si(111) interface was found to be primarily Ca–Si bonds with a neutral overlayer containing complete F^-–Ca^{2+}–F^- triple layers.[18,19] The CaF_2(001) surface has a perpendicular dipole moment and the repeat unit consists of Ca^{2+}–F^- double layers.[17] It may therefore be possible to grow APD-free InSb on these polar CaF_2 surfaces. Moreover, fluoride layers are also known to be effective in relieving thermal mismatch stress in heteroepitaxial systems through gliding dislocations.[7,16,17,20] Their low elastic stiffness coefficients, particularly that of BaF_2, can also provide additional strain relief via plastic deformation.[20–22]

Although the fluorides have much larger thermal expansion coefficients than Si, fluoride films cooled to room temperature after high temperature growth on Si generally do not contain cracks.[17] For thick CdTe/CaF_2/Si structures, near vanishing strain was measured in the CdTe layer and the CaF_2/Si interface is believed to be responsible for the strain relief of the entire structure.[7] The low substrate temperatures used for InSb growth should also help to minimize thermal mismatch problems in InSb/fluoride/Si structures.

In this article, we explore the relatively new use of group IIa fluoride buffer layers in the MBE growth of InSb on Si substrates. Detailed reflection high-energy electron diffraction (RHEED) and scanning electron microscopy (SEM) studies on the initial growth of this heteroepitaxial system are presented. The interfacial properties are investigated using x-ray photoelectron spectroscopy (XPS), the crystalline quality is confirmed using high-resolution x-ray diffraction, and the electrical properties of the InSb films are characterized using Hall-effect measurements. We focus on the use of CaF_2 buffer layers grown on Si(111) substrates since this simple structure provides the smoothest starting surface for subsequent InSb deposition. Some preliminary results using BaF_2 buffers and (001)-oriented substrates are also included.

II. EXPERIMENT

MBE growth of InSb/fluoride/Si structures was carried out in an Intevac Gen II system with an analysis chamber

[a]Electronic mail: wliu@phyast.ou.edu

 0021-8979/97/81(4)/1708/7/$10.00 © 1997 American Institute of Physics

Downloaded¬26¬Jun¬2001¬to¬129.15.117.34.¬Redistribution¬subject¬to¬AIP¬license¬or¬copyright,¬see¬http://ojps.aip.org/japo/japcr.jsp

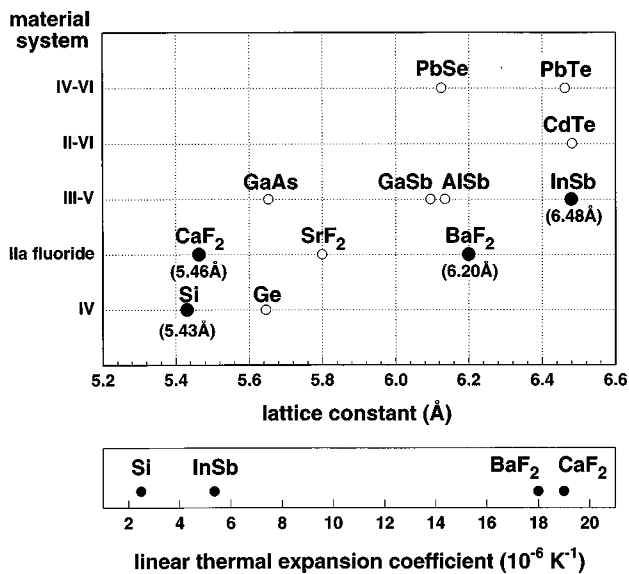

FIG. 1. Lattice constants and thermal expansion coefficients of various material systems related to this work.

and two growth chambers: one for fluoride growth and the other for InSb growth. 3-in.-diameter Si substrates (Silicon Sense, Inc.) were cleaned using the Shiraki method[23] and the passivating oxide was thermally desorbed in the fluoride growth chamber at 1100 °C, producing well-defined Si(111)–(7×7) and 2-domain Si(001)–(2×1) RHEED patterns. Substrate temperatures (T_{sub}) were measured by a thermocouple located at the center of the substrate heater.

High-purity polycrystalline CaF_2 and BaF_2 sources were evaporated independently from graphite-coated PBN crucibles as the Si substrates were rotated at 10 rpm to improve film uniformity. Throughout deposition of the 1000-Å-thick fluoride layers, a background pressure of $\sim 10^{-10}$ Torr was maintained. Typical growth rates for CaF_2 and BaF_2 were approximately 10 and 20 Å/min, respectively, for (111)-oriented growth and 10 Å/min and 15 Å/min, respectively, for (001)-oriented growth. These growth rates correspond to beam equivalent pressures of $\sim 7\times 10^{-8}$ Torr for CaF_2 growth and $\sim 1\times 10^{-7}$ Torr for BaF_2 growth. Substrate temperatures of 700 °C were used for both CaF_2 and BaF_2 growth on Si(111) substrates. For growth on (001)-oriented substrates, CaF_2 was deposited at $T_{sub}\approx 580$ °C and followed by a rapid thermal anneal at 1000 °C to smooth the as-grown surface.[24,25] Details of fluoride growth on Si substrates have been reported elsewhere.[25]

Following fluoride deposition, the samples were cooled to room temperature and transferred under ultra-high vacuum to another growth chamber for subsequent InSb deposition using solid elemental sources of In (7*N*, Nikko Kyodo) and Sb (6.5*N*, Dowa). In most cases, a thin nucleation layer (2000 Å thick) was first grown at a low growth rate ($\sim$0.1 ML/s) and a low temperature ($\sim$300 °C) to reduce the concentration of crystal defects at the interface.[26,27] A T_{sub} from 350 to 400 °C, a growth rate of $\sim$0.65 ML/s, and an Sb_4 to In beam equivalent pressure ratio of $\sim$3 were used for growth of the active layer. Growth rates were inferred from RHEED intensity oscillations observed during InSb growth on GaAs(001) substrates. Growth was interrupted occasionally in the early stages to improve crystallinity and surface smoothness.

A Varian electron gun was operated at 9.5 keV and an angle of incidence between 1° and 3° to monitor the RHEED patterns. Digitized images of these patterns were obtained using a charge-coupled devices (CCD) camera and a data acquisition system developed by *k*-Space Associates, Inc. We have previously demonstrated that RHEED characterization, in spite of the known effects of electron-beam-induced fluorine desorption, can be used to study fluoride surfaces.[25] Electron beam irradiation time on the fluoride layers was kept to a minimum and RHEED patterns recorded at the initial InSb growth stages were taken from previously unexposed areas. These precautions prevent modification of the starting surface by the electron beam and ensure that the observed diffraction features reflect actual growth morphology.

An adjoining analysis chamber was used to conduct XPS experiments at room temperature, thereby eliminating complications associated with the use of capping layers and exposure to atmosphere. The analysis chamber was equipped with a VG100AX hemispherical analyzer and an XR3E2 dual-anode x-ray source used in conjunction with a VGX900 data acquisition system (Fisons Instruments). The base pressure of this chamber was kept below 10^{-9} Torr during the experiments. XPS spectra arising from In $3d$, Sb $3d$, Ca $2p$, and F $1s$ transitions were obtained by running the Al $k\alpha_{1,2}$ source ($h\nu = 1486.6$ eV) at a 15 keV potential and a 10 mA emission current. The constant analyzer energy mode was used with a pass energy of 20 eV.

SEM micrographs were obtained using a JEOL JSM880 system (15 kV potential, $\sim$10 nA emission current) and electron channeling patterns were taken at a 20° scan angle and a 25 kV potential. X-ray diffraction data ($\omega - 2\Theta$ scans) were obtained using a Philips Materials Research Diffractometer operated with a 4-bounce Ge(220) incident-beam monochrometer.

III. RESULTS AND DISCUSSIONS

A. InSb/CaF_2/Si(111)

Figure 2 illustrates the evolution of the RHEED patterns during the growth of InSb/CaF_2/Si(111). The smooth transition from the Si(111)–(7×7) to the CaF_2(111)–(1×1) surface reconstructions [Figs. 2(a) and 2(b)] provides evidence that CaF_2 growth proceeds two-dimensionally. Parallel epitaxy is confirmed by comparing the electron channeling pattern (ECP) of the bare Si substrate with one taken after growth of the CaF_2 film [Figs. 3(a) and 3(b)]. The sixfold symmetry characteristic of (111)-oriented layers is found in both patterns. Fewer details are observed in the CaF_2 pattern as a result of a higher defect density in the CaF_2 layer than in the Si substrate.

Subsequent growth of InSb was initiated by exposing the CaF_2 layer to In and Sb fluxes simultaneously. The emergence of more closely spaced InSb-related spots in the RHEED pattern [Fig. 2(c)] indicated that nucleation took

Downloaded¬26¬Jun¬2001¬to¬129.15.117.34.¬Redistribution¬subject¬to¬AIP¬license¬or¬copyright,¬see¬http://ojps.aip.org/japo/japcr.jsp

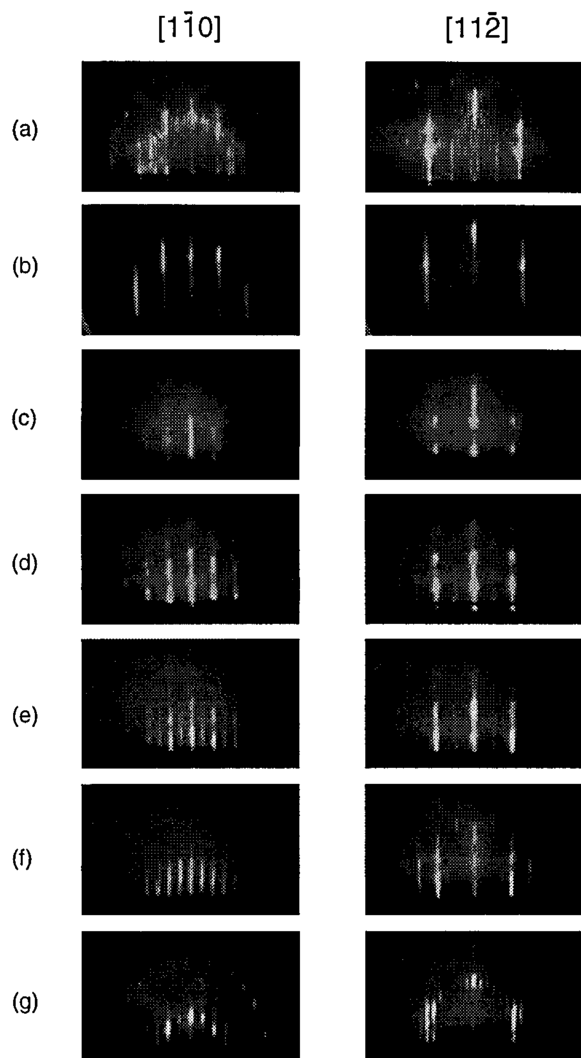

FIG. 2. Evolution of RHEED patterns during the growth of InSb/CaF_2/Si(111): (a) Si(111)–(7×7); (b) 1000 Å CaF_2(111)–(1×1); initial growth of InSb (c) ~2 ML, (d) ~10 ML, (e) ~25 ML; after the growth of a 0.4 μm film showing (f) well-defined InSb(111)–(2×2) and (g) static InSb(111)–(2×6) surface reconstructions.

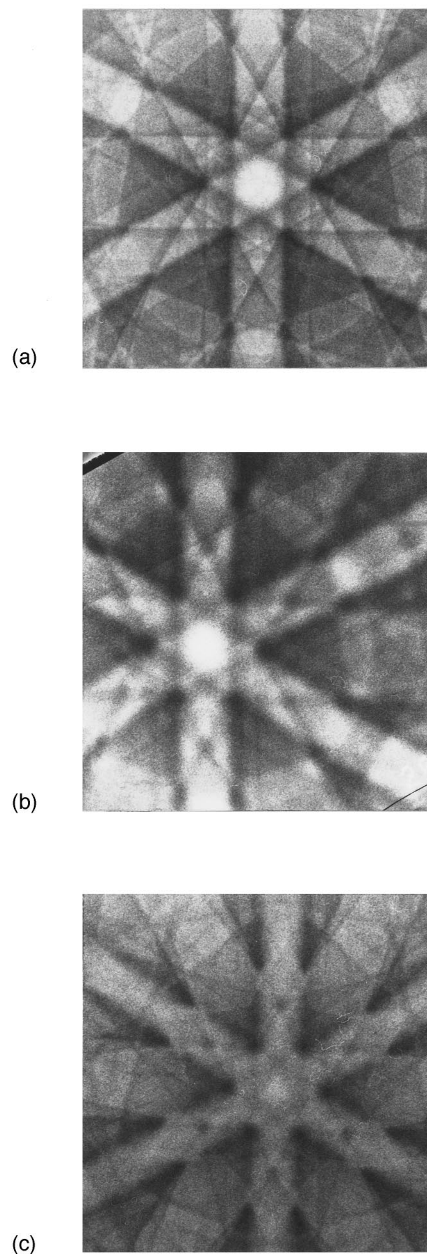

FIG. 3. Electron channeling patterns (25 kV, 20° scan angle) showing the replication of sixfold symmetry in (a) Si(111) substrate, (b) ~1000 Å CaF_2/Si(111) and (c) 8 μm thick InSb/CaF_2/Si(111).

place via the formation of three dimensional (3D) epitaxial islands, as expected from the large lattice mismatch. The cloudy appearance of the sample surface arose from the high density of dislocations at the interface. As growth proceeded, CaF_2 diffraction streaks weakened until disappearing after deposition of ~10 ML of InSb [Fig. 2(d)]. Meanwhile, the InSb diffraction features became brighter and 1/2-order spots began emerging in both the [1$\bar{1}$0] and [11$\bar{2}$] azimuths [Fig. 2(d)]. At an equivalent layer thickness of ~25 ML, 1/2-order streaks could be clearly seen [Fig. 2(e)]. The reflectance of the surface also improved at this stage but was not uniform across the 3 in. wafer. The coalescence of differently sized islands with differing degrees of strain relaxation, and hence different lattice constants,[28] may explain these observations. After depositing 1000 Å of InSb, growth was interrupted while the substrate temperature was raised to 375 °C before further growth resumed. Fig. 2(f) shows a well-defined (2×2) RHEED pattern for a 4000 Å InSb film. It is worth noting that InSb films grown without the low-temperature, low-growth-rate buffer appeared less smooth but more uniform. Increasing the initial growth temperature above 375 °C also roughened the surface. When growth was terminated and the substrate temperature lowered under an Sb flux, a change from a (2×2) In-stabilized to a (2×6) Sb-stabilized surface reconstruction was observed [Fig. 2(g)]. This transition was reversible and is characteristic of an In-terminated InSb(111)A surface.[29,30] This behavior differs from that of GaAs grown on CaF_2/Si(111), where an As-terminated (111)B surface is produced.[31]

XPS spectra of In 3d, Sb 3d, Ca 2p, and F 1s signals taken at various stages of growth are shown in Fig. 4(a). Within the resolution limit of our XPS system (~1 eV), no interfacial products were detected. As shown in Fig. 4(b), the

Downloaded¬26¬Jun¬2001¬to¬129.15.117.34.¬Redistribution¬subject¬to¬AIP¬license¬or¬copyright,¬see¬http://ojps.aip.org/japo/japcr.jsp

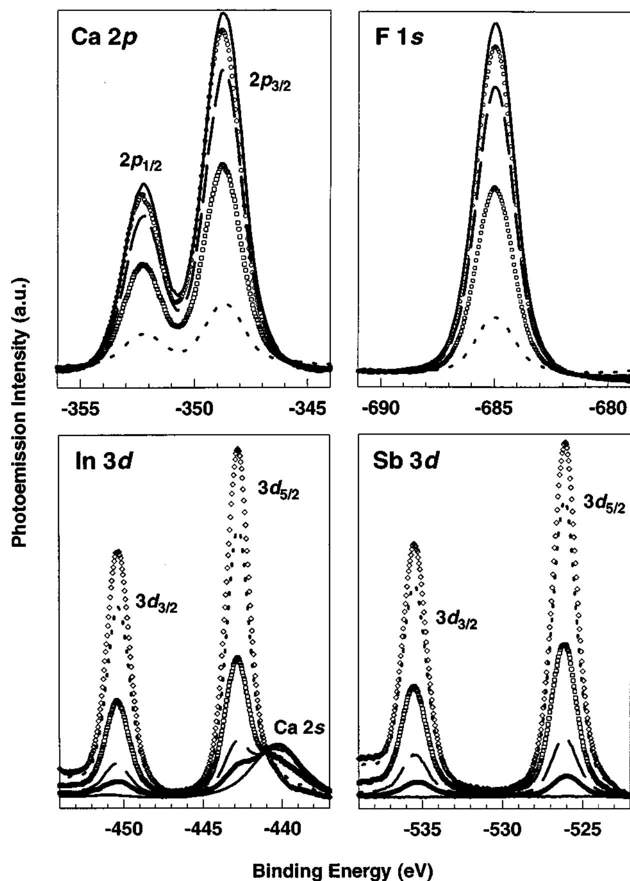

FIG. 4. (a) XPS spectra taken at various stages during the growth of InSb/CaF_2/Si(111); — 1000 Å CaF_2, ○○○ ~1 ML, – – – ~2 ML, □□□ ~7 ML, --- ~25 ML, and ◇ ◇ ◇ 100 ML of InSb; (b) variation of the normalized photoemission intensities of the In $3d$, Sb $3d$, Ca $2p$, and F $1s$ peaks with respect to InSb film thickness.

normalized photoemission intensities of the substrate peaks decrease and the epilayer peaks increase exponentially with increasing InSb coverage. The composition of the InSb film appears stoichiometric throughout the growth.

The crystal quality, epitaxial orientation, and surface morphology of the epilayer were further investigated using SEM and optical microscopy. Nonuniformity in film thickness is detected under SEM by the presence of curved growth steps on an otherwise fairly smooth surface. Optical

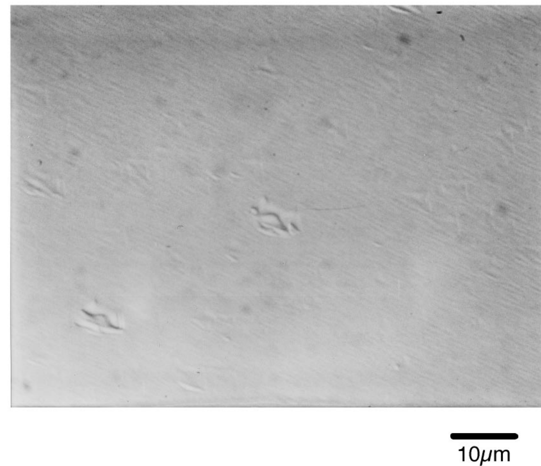

FIG. 5. Nomarski micrograph of an 8 μm thick InSb/CaF_2/Si(111) film revealing the presence of stacking-fault-related features.

micrographs taken under Nomarski interference contrast revealed the presence of features related to stacking faults (Fig. 5). Their density was found to increase dramatically with growth temperature. The initial low-temperature, low-growth-rate buffer also helped reduce the density of these defects. Occasionally, extended cracks along the $\langle 110 \rangle$ directions were observed hundreds of microns apart in films thicker than several microns. Also, sawtooth-shaped microcracks were observed in such samples to be most pronounced around defects and can be attributed to the pinning of strain-relieving misfit dislocations.[17] The sharpness and sixfold symmetry of the electron channeling pattern for an 8 μm InSb film [Fig. 3(c)] is similar to that of the underlying CaF_2/Si layer [Fig. 3(b)]. This indicates that {111} parallel epitaxy is achieved and that the InSb layer is not twinned. The high crystalline quality indicated by the channeling pattern was confirmed by x-ray diffraction measurements where the full width at half maximum for the InSb layer was 125 arcsec. This value is comparable to that reported for material systems with similar lattice mismatch such as CdTe/Si.[2]

To assess the electrical properties of the InSb layers, Hall-effect measurements were carried out at room temperature and 77 K. All samples were found to be n-type with room-temperature mobilities in the 10^4 $cm^2/V\,s$ range. Room temperature electron mobility of $\sim$65 000 $cm^2/V\,s$ ($n \approx 2 \times 10^{16}$ cm^{-3}) was obtained in an 8 μm film grown with a 0.3 μm low-temperature, low-growth-rate buffer. This is as high as any value reported to date for any heteroepitaxial InSb film, regardless of the amount of lattice mismatch.[8,11,12,32–34] A conversion to p-type conduction at low temperature, previously reported for InSb films grown on BaF_2 substrates and attributed to thermal strain,[35] was not observed. The 77 K mobilities, however, were at least an order of magnitude lower than the room temperature values. Similar behavior has been reported for other InSb-on-Si structures and is attributed to electron scattering from dislocations arising from both lattice and thermal strains.[8,10]

The electrical properties of InSb layers with different growth parameters are summarized in Table I. Note that variations in the electrical properties were detected across

Downloaded¬26¬Jun¬2001¬to¬129.15.117.34.¬Redistribution¬subject¬to¬AIP¬license¬or¬copyright,¬see¬http://ojps.aip.org/japo/japcr.jsp

TABLE I. Electrical properties of InSb/fluoride/Si structures studied in this work.

Sample	Structure	Growth parameters[a]	μ_{RT} (cm^2/V s) n_{RT} (cm^{-3})	μ_{77K} (cm^2/V s) n_{77K} (cm^{-3})
S139	InSb/CaF_2/Si(111)	$d_a \approx 2$ μm, $d_b \approx 0.1$ μm, $T_{sub}=375$ °C	24 500–28 500 $n=2.0\times10^{16}$ cm^{-3}	⋯
S140	InSb/CaF_2/Si(111)	$d_a \approx 3$ μm, $d_b \approx 0$ μm, $T_{sub}=375$ °C	13 000 $n=1.9\times10^{16}$ cm^{-3}	⋯
S141	InSb/CaF_2/Si(111)	$d_a \approx 5$ μm, $d_b \approx 0.2$ μm, $T_{sub}=350$ °C	29 020 $n=1.7\times10^{16}$ cm^{-3}	1686 $n=2.3\times10^{15}$ cm^{-3}
S142[b]	InSb/CaF_2/Si(111)	$d_a \approx 0.32$ μm, $d_b \approx 0$ μm, $T_{sub}=300$ °C	47 100 $n=6.1\times10^{17}$ cm^{-3}	18 508–33 137 $n\approx3.9\times10^{16}$ cm^{-3}
S144	InSb/CaF_2/Si(111)	$d_a \approx 8$ μm, $d_b \approx 0.3$ μm, $T_{sub}=350$ °C	48 647–65 518 $n\approx2.0\times10^{15}$ cm^{-3}	4715 $n=1.6\times10^{15}$ cm^{-3}
S145	InSb/BaF_2/CaF_2/Si(111)	$d_a \approx 13$ μm, $d_b \approx 0.1$ μm, $T_{sub}=375$ °C	9820 $n=1.1\times10^{15}$ cm^{-3}	1484 $n=4.5\times10^{15}$ cm^{-3}
S146	InSb/CaF_2/Si(001)	$d_a \approx 4$ μm, $d_b \approx 0.2$ μm, $T_{sub}=375$ °C	9973 $n=2.7\times10^{16}$ cm^{-3}	3638 $n=2.6\times10^{15}$ cm^{-3}

[a] d_a: thickness of active InSb layer, d_b: thickness of low-temperature, low-growth rate InSb buffer.
[b] For XPS studies.

each wafer due to the nonuniform epitaxial growth expected in a system with such a large lattice mismatch. In general, smoother areas yielded higher electron mobilities. The anomalously high 77 K mobility observed for sample S142 may be related to the thinness of the InSb film and the frequent growth interrupts and the thermal cycling occurring between growth temperature and room temperature used for XPS studies. We suspect that the alternating thermal strain field arising from thermal cycling may have acted as a dislocation filter and forced threading dislocations to bend over and propagate parallel to the epilayer.[36] This could result in a reduced dislocation density and hence less electron scattering.

It has been reported that only a very narrow growth window exists for optimal GaAs/CaF_2 films grown on on-axis Si(111) substrates.[31,37,38] The stringent requirement for optimal growth, however, can be relaxed by growing on off-axis substrates.[36,37] In addition, the initial nucleation of GaAs can be improved by the formation of an As layer on the CaF_2/Si(111) surface.[31,39,40] The epitaxial quality of InSb/CaF_2/Si(111) may also be improved by applying an Sb soak prior to growth on off-axis substrates.

B. InSb/BaF_2/CaF_2/Si(111)

It can be inferred from Fig. 1 that the large lattice mismatch between InSb and Si may be better accommodated by using a stacked BaF_2/CaF_2 buffer. The growth of high quality PbSe and CdTe using this structure has been reported.[2–4,7,15,20] We have carried out some preliminary work on the growth of InSb/BaF_2/CaF_2/Si(111) structures. A 1000-Å-thick layer of BaF_2 was deposited immediately after growing the CaF_2 layer. Despite the 14% mismatch between the two fluorides, two-dimensional growth is indicated by the smooth transition from CaF_2(111)–(1×1) to more closely spaced BaF_2(111)–(1×1) RHEED streaks [Fig. 6(a) and 6(b)].

The nucleation of InSb on BaF_2 started by island formation and the InSb surface exhibited a (2×2) reconstruction, similar to the growth of InSb on CaF_2 discussed above. However, the emergence of 1/2-order diffraction features [Fig. 6(c)] was much faster in this case (~2 ML). This suggests that the initial growth is made smoother by reducing the lattice mismatch from >19% to ~4.5% through insertion of the BaF_2 layer. On the other hand, the transition from spotty to streaked RHEED patterns did not occur until over 100 ML of InSb was deposited [Fig. 6(d)]. A (2×2) surface reconstruction was eventually observed [Fig. 6(e)]. The SEM mi-

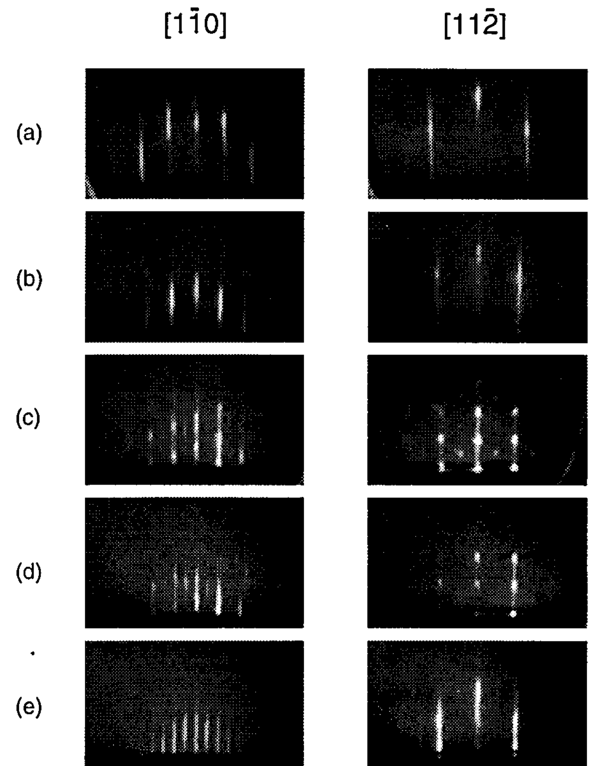

FIG. 6. Evolution of RHEED patterns during the growth of InSb/BaF_2/CaF_2/Si(111): (a) 1000 Å CaF_2(111)–(1×1); (b) 1000 Å BaF_2(111)–(1×1); after the growth of (c) ~2 ML, (d) 100 ML, and (e) 0.1 μm of InSb showing a (2×2) surface reconstruction.

Downloaded¬26¬Jun¬2001¬to¬129.15.117.34.¬Redistribution¬subject¬to¬AIP¬license¬or¬copyright,¬see¬http://ojps.aip.org/japo/japcr.jsp

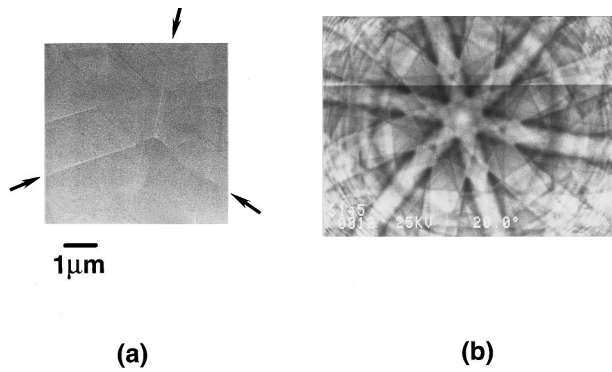

FIG. 7. (a) SEM micrograph of a 13 μm $InSb/BaF_2/CaF_2/Si(111)$ film revealing a relatively smooth surface with shallow triangular steps believed to be related to {100}⟨110⟩-type glide steps and (b) corresponding ECP pattern showing the presence of (111)-related sixfold symmetry and ring structures along the edges.

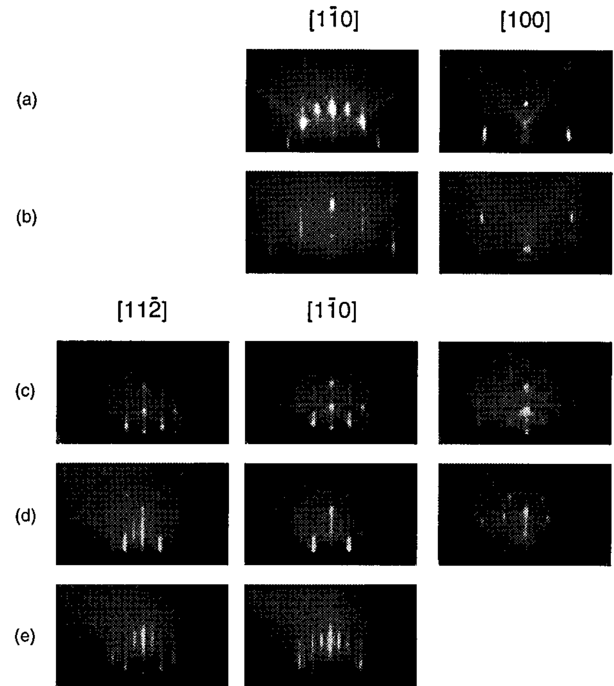

FIG. 8. Evolution of RHEED patterns during the growth of $InSb/CaF_2/Si(001)$: (a) Si(001)–(2×1)+(1×2) and (b) 1000 Å as-grown $CaF_2(001)$–(1×1), taken in the fluoride growth chamber; (c)–(e): after the growth of 60 ML, 0.1 μm and 4 μm of InSb, respectively, taken in the InSb growth chamber with a different camera length for the RHEED setup.

crograph shown in Fig. 7(a) revealed a fairly smooth surface with shallow triangular steps that are probably related to the {100}⟨110⟩-type glide steps commonly observed in the $BaF_2/CaF_2/Si(111)$ system.[21] Although cracks are absent in this system, curved growth steps related to non-uniform growth rate can still be seen. The presence of ring structures along the edges of the ECP pattern of a 13 μm film [Fig. 7(b)] indicated that the crystalline quality of the InSb film deteriorated with the insertion of the BaF_2 layer. One possible cause may be the presence of twinned (type A and B) BaF_2 grains in the buffer layer.

The reduction in lattice mismatch also does not result in improved electrical properties. The unintentionally doped InSb films were n-type with Hall mobilities of ~10 000 cm^2/V s and ~1500 cm^2/V s at room temperature and 77 K, respectively (see Table I). Interdiffusion has been reported for an $InSb/BaF_2$ sandwich-type structure[10] and could lead to the low mobility observed in our layers. In addition, the growth parameters in our initial study have not been optimized for InSb growth on BaF_2 surfaces. For example, the thicknesses of the two fluoride layers were found to be critical for heteroepitaxy of high quality IV–VI layers and the best results were obtained with much thinner CaF_2 layers (<100 Å).[7] Further work will likely improve the epitaxial quality of these structures.

C. $InSb/CaF_2/Si(001)$

Since (001) is the preferred substrate orientation for device applications and the hydroscopic nature of BaF_2 may complicate processing procedures, we have made an initial attempt to grow InSb on CaF_2-coated Si(001) substrates. Due to the presence of a dipole moment perpendicular to the (001) plane and the resulting high surface energy, as grown $CaF_2/Si(001)$ layers tend to have a high density of {111}-oriented facets.[17,25] In order to achieve a smooth surface, an *in situ* rapid thermal annealing procedure[24,25] was applied before transferring the sample at room temperature to the InSb growth chamber. Figs. 8(a) and 8(b) show the RHEED patterns of a clean Si(001) substrate and an annealed $CaF_2(001)$ film, respectively. The growth parameters for InSb were chosen to be the same as for (111)-oriented growth and may not be optimal.

The growth of InSb proceeded with the appearance of 3D spots [Fig. 8(c)] that developed into 2× streaks [Figs. 8(d) and 8(e)] in the [1$\bar{1}$0] azimuth. Identical 2× patterns were seen repeating every 30°. Diffraction features in the [100] azimuth weakened after growth commenced and remained spotty throughout growth. As shown in Fig. 8(c), both the [1$\bar{1}$0] and [11$\bar{2}$] patterns indicate a superposition of two surface structures and contain double diffraction and twinning spots. This suggests that InSb grows in the (111) orientation with two domains 90° apart, corresponding to the epitaxial relationship:

$$(111)\mathrm{InSb}\|(001)\mathrm{CaF}_2,$$

$$[11\bar{2}]\mathrm{InSb}\|[1\bar{1}0]\mathrm{CaF}_2 \text{ or } [11\bar{2}]\mathrm{InSb}\|[110]\mathrm{CaF}_2.$$

The above relationship is consistent with the observed ECP pattern dominated by ring structures and containing both (111)-related sixfold symmetry and (001)-related fourfold symmetry. Such misoriented growth may be favored since growth in the InSb [11$\bar{2}$] direction reduces the lattice mismatch from ~19% to <3%. The same phenomenon is also encountered in CdTe growth on Si(001) and GaAs(001) substrates.[5,6,41–43] As expected, the crystalline quality and electrical properties of these twinned films were worse than those grown on (111)-oriented substrates (see Table I).

As mentioned before, these $InSb/CaF_2/Si(001)$ structures were probably not grown under optimum conditions. It is

Downloaded¬26¬Jun¬2001¬to¬129.15.117.34.¬Redistribution¬subject¬to¬AIP¬license¬or¬copyright,¬see¬http://ojps.aip.org/japo/japcr.jsp

widely believed that whether CdTe(001) or CdTe(111) is obtained on Si(001) and GaAs(001) substrates depends critically on the starting substrate surface.[6,43] In an earlier work,[25] we reported that (001) parallel epitaxy for BaF_2 can only be achieved on unannealed, and therefore rough, CaF_2/Si(001) surfaces. It is thus possible that the high-temperature smoothing procedure applied to the CaF_2/Si(001) surface may be detrimental to subsequent InSb growth. Further studies are necessary to establish the optimal growth conditions for high quality InSb/CaF_2/Si(001) structures.

IV. CONCLUSIONS

The epitaxial growth of InSb on large lattice-mismatch Si substrates was achieved by MBE using CaF_2 and stacked BaF_2/CaF_2 buffer layers. Structural and room-temperature electrical data indicate that Si can be used as a substrate for InSb growth. However, detailed study of the influence of growth parameters such as substrate orientation, shutter opening sequence, flux ratio, growth temperature, and buffer layer thickness on the crystal quality need to be done before the prospect of growing vertically stacked single-crystal narrow-gap compound semiconductor/insulator/Si structures can be realized.

ACKNOWLEDGMENTS

The authors thank Matthew Johnson for helpful discussion, Bill Chissoe for the SEM studies, and Joel Young for technical support. This work is supported by the NSF through Grant Nos. OSR-9108771, OSR-9550478 and ECS-9410015.

[1] Y. Lo, R. N. Bicknell, T. H. Myers, J. F. Schetzina, and H. H. Stadelmaier, J. Appl. Phys. **54**, 4248 (1983).
[2] H. Zogg and S. Blunier, Appl. Phys. Lett. **49**, 1531 (1986).
[3] A. N. Tiwari, W. Floeder, S. Blunier, H. Zogg, and H. Weibel, Appl. Phys. Lett. **57**, 1108 (1990).
[4] A. N. Tiwari, S. Blunier, and H. Zogg, Appl. Phys. Lett. **60**, 621 (1992).
[5] R. Sporken, S. Sivananthan, K. K. Mahavadi, G. Monfroy, M. Boukerche, and J. P. Faurie, Appl. Phys. Lett. **55**, 1879 (1989).
[6] J. P. Faurie, R. Sporken, S. Sivananthan, and M. D. Lange, J. Cryst. Growth **111**, 698 (1991).
[7] H. Zogg, S. Blunier, and J. Masek, J. Electrochem. Soc. **136**, 775 (1989).
[8] J.-I. Chyi, D. Biswas, S. V. Iyer, N. S. Kumar, H. Morkoc, R. Bean, K. Zanio, H.-Y. Lee, and Haydn Chen, Appl. Phys. Lett. **54**, 1016 (1989).
[9] G. E. Franklin, D. H. Rich, Hawoong Hong, T. Miller, and T.-C. Chiang, Phys. Rev. B **45**, 3426 (1992).
[10] H. C. Lu, H. R. Fetterman, C. J. Chen, C. Hsu, and T. M. Chen, Solid-State Electron. **36**, 533 (1993).
[11] L. K. Li, Y. Hsu, and W. I. Wang, J. Vac. Sci. Technol. B **11**, 872 (1993).
[12] S. V. Ivanov, A. A. Boudza, R. N. Kutt, N. N. Ledentsov, B. Ya. Meltser, S. S. Ruvimov, S. V. Shaposhnikov, and P. S. Kop'ev, J. Cryst. Growth **156**, 191 (1995).
[13] T. Sudersena Rao, J. B. Webb, D. C. Houghton, J. M. Baribeau, W. T. Moore, and J. P. Noad, Appl. Phys. Lett. **53**, 51 (1988).
[14] W. Dobbelaere, J. De Boeck, and G. Borghs, Appl. Phys. Lett. **55**, 1856 (1989).
[15] H. Zogg and M. Hüppi, Appl. Phys. Lett. **47**, 133 (1985).
[16] H. Zogg, C. Maissen, S. Blunier, S. Teodoropol, R. M. Overney, T. Richmond, and J. W. Tomm, Semicond. Sci. Technol. **8**, S337 (1993).
[17] Leo J. Schowalter and Robert W. Fathauer, CRC Crit. Rev. Solid State Mater. Sci. **15**, 367 (1989), and references therein.
[18] F. J. Himpsel, F. U. Hillebrecht, G. Hughes, J. L. Jordan, U. O. Karleson, F. R. McFeely, J. F. Morar, and D. Rieger, Appl. Phys. Lett. **48**, 596 (1986).
[19] Marjorie A. Olmstead, R. I. G. Uhrberg, R. D. Bringans, and R. Z. Bachrach, J. Vac. Sci. Technol. B **4**, 1123 (1986).
[20] H. Zogg, Appl. Phys. Lett. **49**, 933 (1986).
[21] S. Blunier, H. Zogg, C. Maissen, A. N. Tiwari, R. M. Overney, H. Haefke, P. A. Buffat, and G. Kostorz, Phys. Rev. Lett. **68**, 3599 (1992).
[22] P. W. Sullivan, R. F. C. Farrow, and G. R. Jones, J. Cryst. Growth **60**, 403 (1982).
[23] A. Ishizaka and Y. Shiraki, J. Electrochem. Soc. **133**, 666 (1986).
[24] T. Asano, H. Ishiwara, and S. Furukawa, Jpn. J. Appl. Phys. **27**, 1193 (1988).
[25] X. M. Fang, P. J. McCann, and W. K. Liu, Thin Solid Films **272**, 87 (1996).
[26] G. M. Metze and A. R. Calawa, Appl. Phys. Lett. **42**, 818 (1983).
[27] K. Ishida, M. Akiyama, and S. Nichi, Jpn. J. Appl. Phys. **25**, L288 (1986).
[28] S. J. Rosner, S. M. Koch, and J. S. Harris, Jr., Appl. Phys. Lett. **42**, 1764 (1986).
[29] A. J. Noreika, M. H. Francombe, and C. E. C. Wood, J. Appl. Phys. **52**, 7416 (1981).
[30] T. Nakada, T. Ikeda, M. Yata, and T. Osaka, Surf. Sci. **222**, L825 (1989).
[31] W. Li, T. Anan, and L. J. Schowalter, J. Cryst. Growth **135**, 78 (1994).
[32] J.-I. Chyi, S. Kalem, N. S. Kumar, C. W. Litton, and H. Morkoc, Appl. Phys. Lett. **53**, 1092 (1988).
[33] J. R. Söderström, M. M. Cumming, J.-Y. Yao, and T. G. Andersson, Semicond. Sci. Technol. **7**, 337 (1992).
[34] G. S. Lee, P. E. Thompson, J. L. Davis, J. P. Omaggio, and W. A. Schmidt, Solid-State Electron. **36**, 387 (1993).
[35] John L. Davis, Thin Solid Films **192**, 111 (1990).
[36] G. W. Turner, *Semiconductor-based Heterostructures: Interfacial Structure and Stability*, edited by M. L. Green, J. E. E. Baglin, G. Y. Chin, H. W. Deckman, W. Mayo, and D. Narasinham (Metallurgical Society, Pennsylvania, 1986).
[37] H. Mizukami, K. Tsutsui, and S. Furukawa, Jpn. J. Appl. Phys. **30**, 3349 (1991).
[38] W. Li, T. Thundat, T. Anan, and L. J. Schowalter, J. Vac. Sci. Technol. B **13**, 670 (1995).
[39] W. Li, T. Anan, and L. J. Schowalter, J. Vac. Sci. Technol. B **12**, 1067 (1994).
[40] W. Li, T. Thundat, T. Anan, and L. J. Schowalter, Appl. Phys. Lett. **65**, 595 (1994).
[41] H. A. Mar, N. Salansky, and K. T. Chee, Appl. Phys. Lett. **44**, 898 (1984).
[42] J. M. Ballingall, W. J. Takei, and Bernard J. Feldman, Appl. Phys. Lett. **47**, 599 (1985).
[43] J. P. Faurie, C. Hsu, S. Sivananthan, and X. Chu, Surf. Sci. **168**, 473 (1986).

Downloaded¬26¬Jun¬2001¬to¬129.15.117.34.¬Redistribution¬subject¬to¬AIP¬license¬or¬copyright,¬see¬http://ojps.aip.org/japo/japcr.jsp